ACADEMIC PRESS

Available online at www.sciencedirect.com

SCIENCE DIRECT®

VIROLOGY

Virology 311 (2003) 241–253

www.elsevier.com/locate/yviro

Structural determinants of insert retention of poliovirus expression vectors with recombinant IRES elements

Elena Y. Dobrikova, Paola Florez, and Matthias Gromeier*

Department of Molecular Genetics and Microbiology, Duke University Medical Center, Durham, NC 27710, USA

Received 7 August 2002; returned to author for revision 18 September 2002; accepted 2 January 2003

Abstract

Although picornaviruses provide attractive vectors for expression of foreign genes, poor genetic stability restricts their use for immunization purposes. A new prototype vector was generated to increase foreign insert retention, by shifting of the initiation codon to a cryptic AUG within the internal ribosomal entry site (IRES) and replacement of IRES domain VI with foreign ORFs. Using our strategy to replace regulatory noncoding sequences with unrelated foreign genetic material, we generated stable poliovirus-based expression vectors with robust long-term expression of foreign ORFs. Our studies revealed that size and predicted secondary structure formed by the heterologous sequences govern long-term retention and efficiency of expression of foreign inserts replacing IRES structures. These observations indicate that, with certain limitations imposed by structural preferences, foreign sequences can functionally replace IRES substructures in stable picornavirus immunization vectors.

Keywords: Poliovirus; Vaccine; IRES; HIV; SIV

Introduction

Due to the emerging threat of spreading infectious disease, either incidental or intentional, the design of novel immunization vehicles has become an urgent priority. The danger arising from the possibility of deliberate exposure of populations to a wide array of infectious agents requires flexible vaccination strategies that can be adjusted for prophylaxis against a variety of agents in a short period of time.

Live-attenuated viral vaccine vectors represent a key technology to provide the appropriate means to meet these new challenges. Live viral vectors, manipulated through insertion of heterologous genetic material from various sources, can easily be directed against diverse infectious agents. In many instances, they can be mass-produced at low cost and generally require simple, noninvasive means of administration.

In the recent past, a number of live-attenuated viruses were investigated as possible immunization vectors against infectious diseases. Among these, picornaviruses, especially poliovirus, played a central role. The molecular biology of picornaviruses is thoroughly understood and numerous strategies for genetic manipulation have produced a rich repertoire of candidate vectors (see Fig. 1). Most importantly, the success of the live-attenuated poliovirus (Sabin) strains used for vaccination for decades indicates the potential for picornavirus-based vaccination vectors (Melnick, 1993; Gromeier et al., 1997).

Several strategies were developed to express foreign genes or gene fragments in a picornavirus background (Fig. 1). These included minor insertions into the coding region for the capsid proteins to display antigenic epitopes on the surface of the viral capsid (Fig. 1B). The insert size with capsid display vectors is limited to a few amino acids (Fig. 1B) (Burke et al., 1989; Evans et al., 1989; Arnold et al., 1996; Halim et al., 2001). Manipulation of the capsid exterior invariably is associated with decreased virus viability and may trigger adaptation events that eliminate the foreign insert to restore proper growth. A second strategy yielding

* Corresponding author. Dept. of Molecular Genetics & Microbiology, Duke University Medical Center, Box 3020, Durham, NC 27710. Fax: +1-919-684-8735.

E-mail address: grome001@mc.duke.edu (M. Gromeier).

0042-6822/03/$ – see front matter © 2003 Elsevier Science (USA). All rights reserved.
doi:10.1016/S0042-6822(03)00191-0

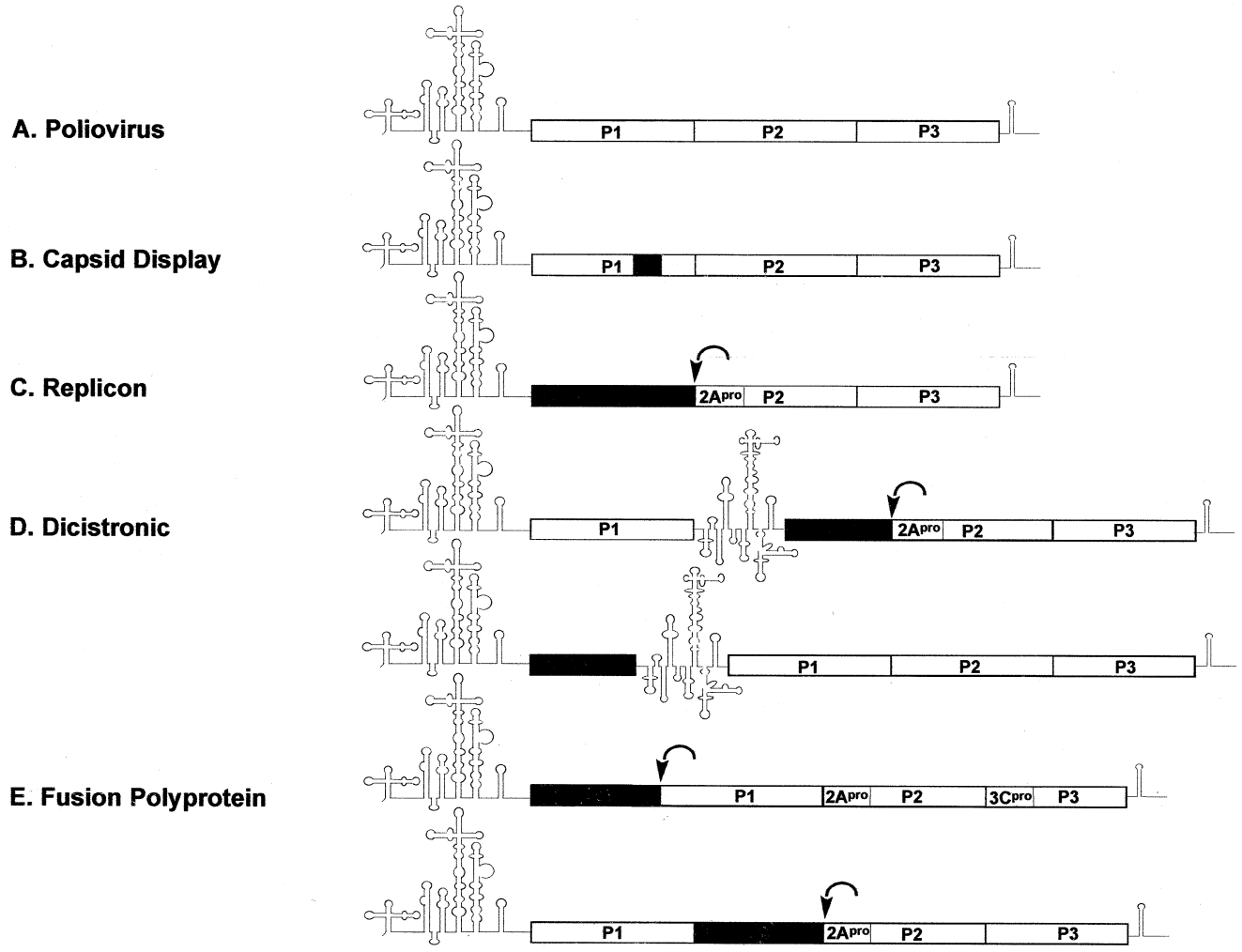

Fig. 1. The genetic structure of proposed picornavirus expression vectors. The predicted secondary structure of 5′- and 3′-noncoding regions is indicated and the major proteolytic products of the viral polyprotein (P1, P2, and P3) are outlined by open boxes. Solid boxes represent heterologous inserts. Engineered proteolytic cleavage sites for the viral proteinases $2A^{pro}$ and $3C^{pro}$, respectively, are indicated by curved arrows. (A) Wild-type poliovirus. (B) Capsid display vectors (Burke et al., 1989; Evans et al., 1989; Arnold et al., 1996; Halim et al., 2001) contain minor foreign inserts within the P1 region (coding for the structural proteins). (C) Poliovirus replicons were generated by replacing the entire coding region for P1 with a foreign ORF (Burke et al., 1989; Choi et al., 1991; Porter et al., 1995). (D) Dicistronic vectors. Foreign ORFs were placed under control of a secondary (encephalomyocarditis; EMCV) IRES element and inserted between P1 and P2 (Lu et al., 1995). Alternatively, the upstream cistron is formed by the foreign ORF driven by the poliovirus IRES, and the viral polyprotein is expressed under control of the EMCV IRES (Alexander et al., 1994). (E) Polyprotein fusion vectors. Foreign sequences were fused to the viral ORF at its 5′ terminus (Andino et al., 1994) or between the coding regions for P1 and P2 (Tang et al., 1997; Crotty et al., 1999, 2001). Both artificial proteolytic cleavage sites for the viral $2A^{pro}$ (Crotty et al., 1999, 2001) and $3C^{pro}$ (Andino et al., 1994; Tang et al., 1997; Mueller et al., 1998) proteinases have been utilized for proteolytic processing of the fusion polyprotein.

replicons was based on the replacement of the structural genes with heterologous open reading frames (ORF) (Fig. 1C) (Burke et al., 1989; Choi et al., 1991; Porter et al., 1995). In the case of replicons, the stringent size limitations were overcome, but resulting viruses were replication defective and required capsid protein-expression systems to be supplied in *trans* for vector propagation.

The third strategy generated dicistronic constructs in which the foreign ORFs were placed under translational control of a secondary heterologous internal ribosomal entry site (IRES) yielding replication competent viruses with independent expression of foreign and viral genes (Fig. 1D) (Alexander et al., 1994; Lu et al., 1995).

Most recently, polyprotein fusion vectors were developed in which the foreign ORF was linked to the viral polyprotein with proteolytic processing provided through an artificial cleavage site for virally encoded proteinases (Fig. 1E) (Andino et al., 1994; Tang et al., 1997; Crotty et al., 1999, 2001).

A major limitation for use as expression vectors common to all replication-competent (+)-strand RNA viruses is their poor genetic stability. Any attempt to achieve long-term expression of foreign genetic material was confronted with the phenomenon of gradual deletion of the heterologous sequences from the viral genome in subsequent passages (Alexander et al., 1994; Lu et al., 1995; Mueller and Wim-

mer, 1998; Dufresne et al., 2002). In most instances, heterologous ORFs were lost almost entirely within three generations upon replication in HeLa cells after transfection of infectious RNA (Mueller and Wimmer, 1998; Dufresne et al., 2002).

Attempts to increase genetic stability by varying the insertion locale did not significantly alter retention rates of foreign ORFs. Dicistronic and polyprotein fusion vectors have been generated that contain foreign inserts either fused N-terminally to the viral polyprotein (Figs. 1D and E) (Alexander et al., 1994; Andino et al., 1994), or separating P1 and P2 (Figs. 1D and E) (Lu et al., 1995; Tang et al., 1997; Crotty et al., 1999, 2001).

Here we are proposing a new approach to generate poliovirus-based expression vectors for immunization purposes. Our strategy includes fusion of foreign ORFs to the viral polyprotein through artificial proteolytic cleavage sites (proposed earlier by Andino et al., 1994). However, instead of merely adding foreign sequences to the viral genome, we designed inserts to functionally replace a structural element contained within the IRES. Our strategy to favor retention of heterologous genetic material through strategic placement within a noncoding regulatory element produced expression vectors with improved genetic stability replicating with near wild-type kinetics in HeLa cells. Moreover, we have identified the size limitations and structural requirements for long-term retention and efficient expression of foreign inserts in picornaviral expression vectors with recombinant IRES elements.

Results

PVS-RIPO, a highly attenuated chimeric virus containing the human rhinovirus type 2 (HRV2) IRES in a poliovirus type 1 (Sabin) [PV1(S)] background (Gromeier et al., 1996), was used as the backbone vector to generate poliovirus-based expression constructs. We chose this chimeric virus for our studies because evaluation of neurovirulence of PV1(RIPO) [in a poliovirus type 1 (Mahoney) background] in nonhuman primates revealed levels of attenuation equal to PV1(S) (Gromeier et al., 1999). These observations indicated that attenuation of neurovirulence of PVS-RIPO [containing attenuation determinants mapping to the coding region for the structural gene products and the RNA polymerase $3D^{pol}$ (Gromeier and Nomoto, 2002) in addition to the attenuating effect of the HRV2 IRES] may be superior to that of PV1(S). Comprehensive neurovirulence assessment of PVS-RIPO in nonhuman primates is scheduled to begin in the near future. Moreover, unlike the Sabin vaccine strains, the attenuation phenotype of PVS-RIPO is remarkably stable upon passage in cell lines of neuronal derivation or mice transgenic for the human poliovirus receptor (Gromeier et al., 1996, 2000).

We have used a new approach for the construction of fusion polyprotein expression vectors to increase long-term retention and expression of foreign sequences. Rather than inserting foreign sequences into the intact poliovirus genome, we replaced parts of the HRV2 IRES with heterologous ORFs of varying size. IRESs of all picornaviruses feature highly conserved structure elements predicted to form stable stem-loop domains (Pilipenko et al., 1989a, 1989b; Skinner et al., 1989). These predicted hairpin structures are separated by linear sequence motifs that may display a surprising level of sequence conservation among picornaviruses. For example, a six-nucleotide stretch separating stem-loop domains IV and V is highly conserved throughout the enterovirus and rhinovirus genera and is absolutely required for IRES function (Belov et al., 1995).

The most thoroughly studied sequence motif within picornavirus IRES elements is a conserved linear polypyrimidine stretch located in between stem-loop domains V and VI (Fig. 2) (Iizuka et al., 1989; Meerovitch et al., 1991; Pestova et al., 1991; Pilipenko et al., 1992; Wimmer et al., 1993). The Y(n)X(m)AUG motif contains a cryptic AUG codon that is never used to initiate translation (Pestova et al., 1991; Wimmer et al., 1993). Instead, an AUG triplet located 33 nt (HRV2) or 155 nt (poliovirus) downstream of Y(n)X(m)AUG serves as initiation codon for the viral polyprotein synthesis (Fig. 2A). It has been previously shown for poliovirus (Pestova et al., 1994) that initiation of translation can be moved to Y(n)X(m)AUG by altering the context of its AUG triplet. We deleted stem-loop domain VI of the HRV2 IRES and placed the Y(n)X(m)AUG in Kozak context (Fig. 2B; Kozak, 1999). This manipulation yielded a viable virus, RPδ6, which exhibited replication kinetics in HeLa cells similar to the parental PVS-RIPO virus (Fig. 2C), suggesting that deletion of IRES domain VI only had a minor effect on virus growth.

RPδ6 was used as the backbone vector to generate poliovirus-based expression constructs with heterologous ORFs (Fig. 3). Foreign genes were inserted immediately downstream of the Y(n)X(m)AUG motif, which supplied the initiation codon for the fusion polyprotein (Fig. 3A). The sequence encoding the N-terminal four amino acids of the polioviral polyprotein (MGAQ. . .) was placed at the 5′ junction of the expression cassette to ensure proper processing of the fusion polyprotein (Fig. 3A). The 3′ junction of the foreign insert and the polioviral ORF contained the sequence encoding an artificial cleavage site for the viral proteinase 2A ($2A^{pro}$; . . .KGLTTY'G. . .; Fig. 3A) (Andino et al., 1994; Crotty et al., 1999). Thus, posttranslational proteolytic cleavage of the fusion polyprotein was predicted to release foreign and viral polypeptides without impediment to virus viability.

A series of expression constructs were generated to evaluate our approach. First, we tested the influence of insert size on genetic stability (Fig. 3). For this purpose, RPδ6 expression vectors containing inserts encompassing the ORFs of a bacterial antigen (a portion of *Escherichia coli* FimH; 102 nt), the human immunodeficiency virus tat protein (HIV_{tat}; 282 nt), simian immunodeficiency virus matrix

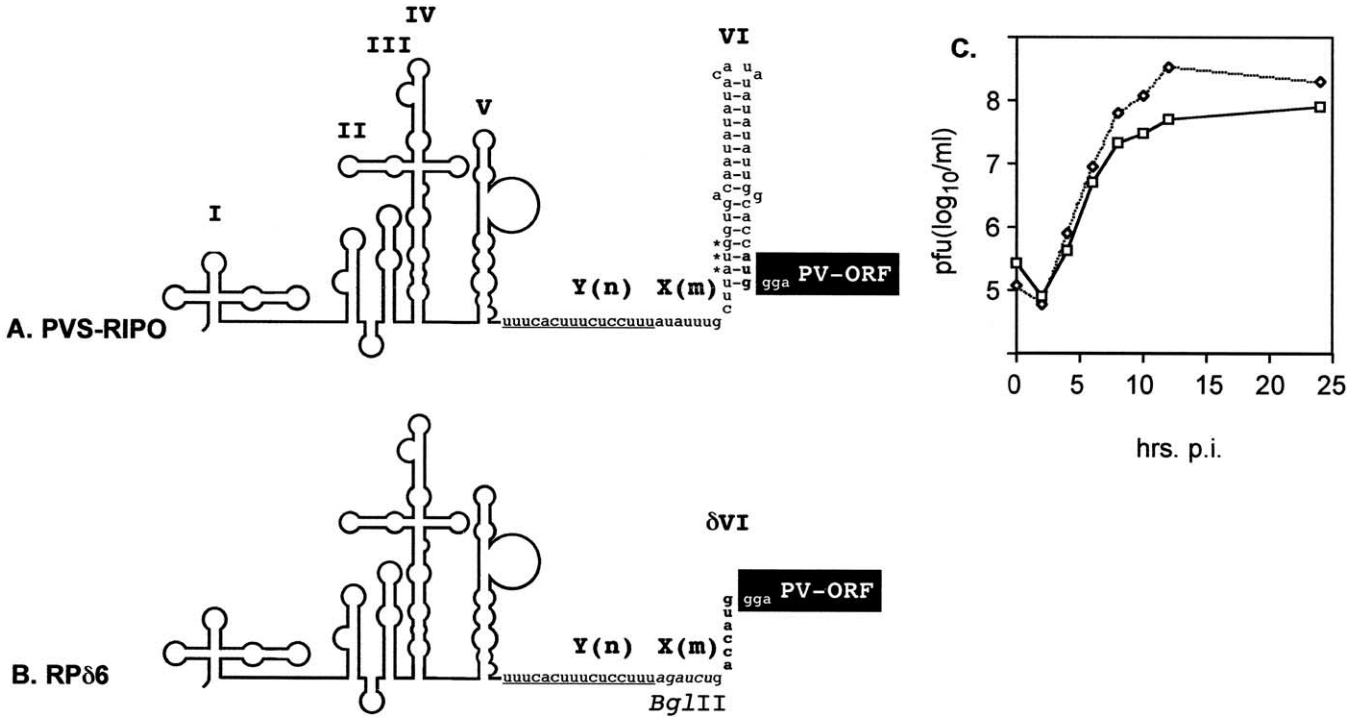

Fig. 2. Genetic structure and growth properties of PVS-RIPO and a deletion variant. (A) PVS-RIPO contains a full-length HRV2 IRES element. The polypyrimidine tract [Y(n)], separating stem-loop domains V and VI, is underlined. The conserved cryptic AUG is indicated by asterisks and separated from Y(n) by a spacer [X(m)]. Initiation of translation occurs at an AUG codon (bold) located 33 nt downstream of the cryptic AUG within Y(n)X(m)AUG. (B) In the deletion mutant (RPδ6), the sequence of X(m) was altered to incorporate a restriction site for endonuclease *Bgl*II and to place the cryptic AUG in Kozak context (. . .cuu**aug**. . . to acc**aug**. . .). The remainder of IRES domain VI was deleted and translation in RPδ6 started from Y(n)X(m)AUG. (C) Comparison of the growth properties of the parental PVS-RIPO (open diamonds) with those of RPδ6 (open squares) in HeLa cells in one-step growth curves.

protein (SIV_{p17}; 420 nt), and the enhanced green fluorescent protein (EGFP; 744 nt), respectively, were generated (Figs. 3A–D). The insert length indicated comprises sequences coding for the leader peptide and the artificial proteolytic cleavage site in addition to the foreign ORF.

The 5′-terminal sequences of the foreign inserts in RPδ6-FimH, RPδ6-HIV_{tat}, and RPδ6-EGFP were modified by silent mutagenesis to form a predicted stable stem-loop structure in a position equal to HRV2 IRES domain VI (see sequence detail in Figs. 3A, B, and D). RPδ6-SIV_{p17}, by virtue of the presence of the "AUG" loop in the SIV 5′ leader (Berkhout, 1996), naturally formed a stable stem-loop structure reminiscent of the HRV2 IRES domain VI (Fig. 3C).

All four expression constructs produced viable viruses, but insert retention through serial passages in HeLa cells varied dramatically (Figs. 3A–D). Whereas RPδ6-FimH (102 nt insert) and RPδ6-HIV_{tat} (282 nt insert) retained the full-length insert throughout at least 20 subsequent passages (Figs. 3A and B), expression constructs containing larger foreign ORFs were less stable. Serial passage of RPδ6-SIV_{p17} (420 nt insert) revealed the emergence of deletion variants nine passages after transfection, and foreign sequences within RPδ6-EGFP (744 nt insert) were deleted already during the first passage (Fig. 3D).

The evaluation of long-term insert retention of all expression vectors by RT-PCR analysis was complemented by plaque assays of each individual passage. Apart from the results of RT-PCR analysis, deletion events after passaging of RPδ6-SIV_{p17} and RPδ6-EGFP were also evident by the emergence of large-plaque variants. In contrast, the plaque phenotype of the stable RPδ6-FimH and RPδ6-HIV_{tat} remained constant throughout 20 passages (data not shown).

Our observations may indicate that, within limits, poliovirus expression vectors can be designed to retain foreign ORFs using integration of heterologous inserts into 5′ regulatory elements. Furthermore, our experiments suggest inserts $>$ 300 nt in length may exceed the size restraints imposed by the location of the insert and may trigger deletion events.

To ascertain whether insert retention correlated with the size of the foreign ORF alone, we constructed RPδ6-SIV_{p17}(282) and RPδ6-EGFP(282) (Fig. 4). In both constructs the insert size was adjusted by C-terminal deletion of the foreign ORF to correspond to that of the genetically stable RPδ6-HIV_{tat}(282). Apart from the shortened foreign insert, the genetic structure of RPδ6-SIV_{p17}(282) and RPδ6-EGFP(282) was identical to the unstable RPδ6-SIV_{p17}(420) and RPδ6-EGFP(744) (compare Figs. 3C and D and Figs. 4A and B). The diminished size of the foreign inserts resulted in increased genetic stability, evident by complete insert retention after 20 passages (Fig. 4). Our observations

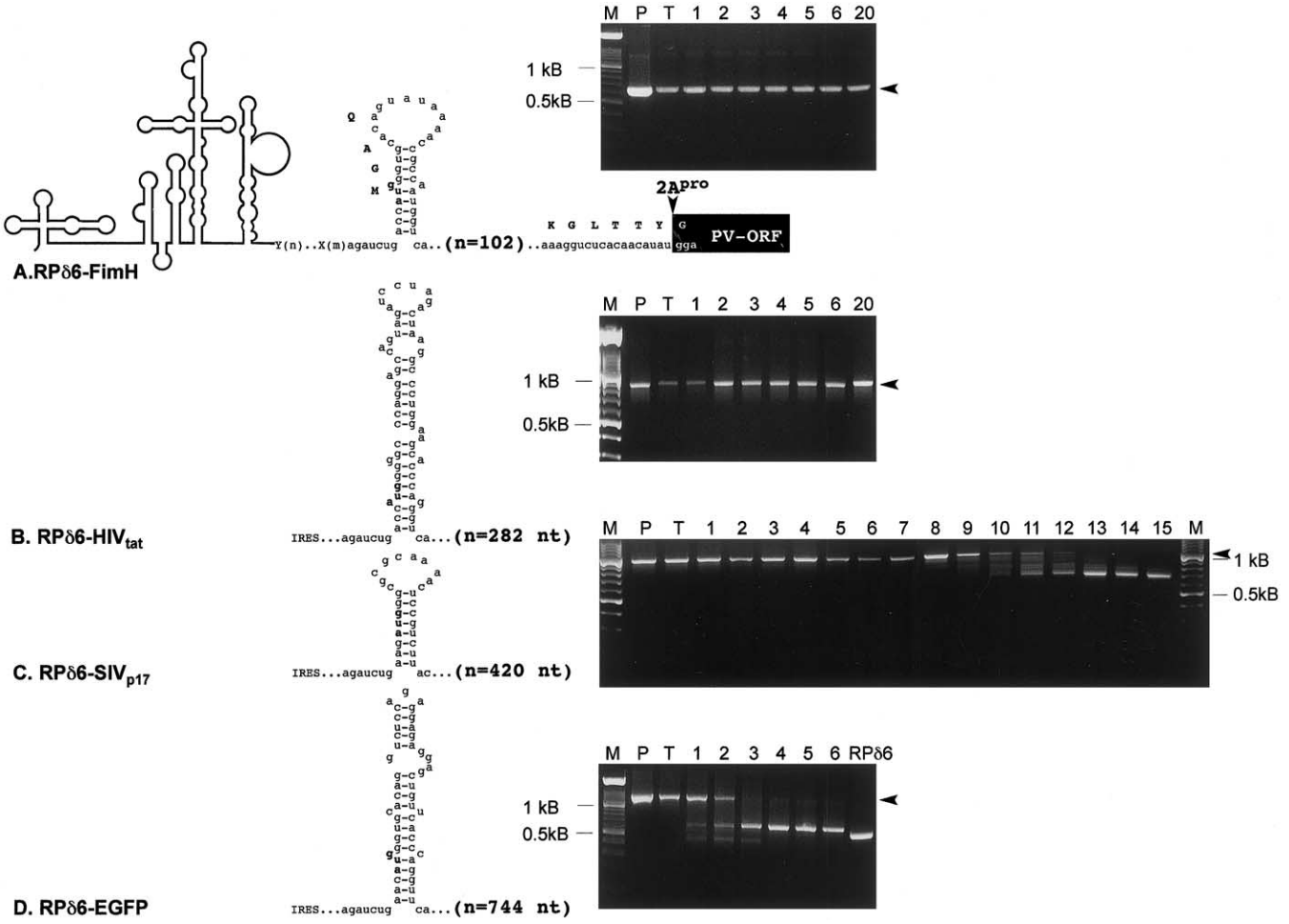

Fig. 3. Genetic structure and stability of RPδ6-based expression vectors with foreign inserts of different sizes. The general architecture of these expression vectors is exemplified by RPδ6-FimH (A). Foreign sequences are inserted in a position to emulate stem-loop domain VI of the HRV2 IRES. The position and amino acid sequence of an artificial cleavage site for $2A^{pro}$ is indicated. The polioviral ORF is represented by a black box. The sequence detail represents the 5′ termini of each of the foreign inserts forming a predicted artificial stem-loop structure replacing IRES domain VI, as shown. The location of the initiating AUG within Y(n)X(m)AUG and the position of the leader peptide are identical in all constructs. The total lengths of the foreign inserts, including sequences of the leader peptide and the artificial proteolytic cleavage site, are shown in bold. The results of RT-PCR analysis of total cellular RNA from infected cultures in serial passages are shown on the right. Labeling of the agarose gels corresponds to the origin of the total RNA preparation subjected to RT-PCR analysis (P = plasmid DNA of the corresponding expression construct; T = RNA isolated from HeLa cells transfected with in vitro transcript; 1–15 = individual virus passages; RPδ6 = plasmid DNA of the backbone construct without any foreign insert; M = molecular weight marker). Arrowheads indicate amplicons corresponding to the full-length inserts. (A) RPδ6 expressing a portion of the bacterial adhesion molecule FimH. (B) RPδ6 expressing the HIV-1 tat protein. (C) RPδ6 expressing the SIV matrix protein (SIV_{p17}). (D) RPδ6 expressing the enhanced green fluorescent protein (EGFP).

confirmed that insert size was the cardinal determinant of foreign ORF retention.

Despite the diminished genetic stability of RPδ6-SIV_{p17} and RPδ6-EGFP, our approach produced prototype expression vectors that exhibited far superior retention of foreign ORFs than previously reported strategies to generate polyprotein fusion vectors. These vectors, independently of insert size, are characterized by a high degree of genetic instability (Mueller and Wimmer, 1998). This was also evident when we constructed “conventional” polyprotein fusion vectors using a blueprint proposed by Andino et al. (1994). Vectors containing a 420-nt SIV_{p17} insert equal to RPδ6-SIV_{p17} fused to the poliovirus ORF and containing the entire IRES element deleted foreign sequences within one to two passages (Dufresne et al., 2002).

Next, we evaluated the influence of predicted secondary structure on insert retention of RPδ6 expression vectors. Since part of our strategy is based on the functional replacement of IRES stem-loop domain VI, the secondary structure assumed by the foreign insert is likely to influence IRES function and, therefore, insert retention. We chose RPδ6-SIV_{p17} to alter the predicted stability of the artificial stem-loop domain VI formed by heterologous sequences (Fig. 5). The initiating AUG codon of SIV_{p17} is located within the AUG loop of the SIV leader in a position similar to that of the cryptic AUG within the Y(n)X(m)AUG motif of picor-

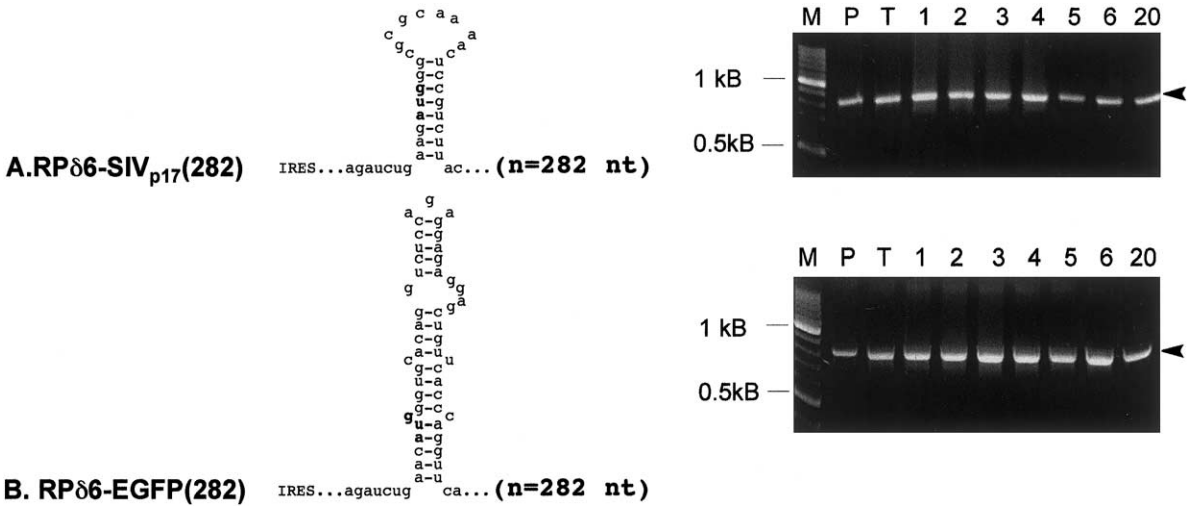

Fig. 4. Genetic structure of RPδ6-SIV$_{p17}$(282) (A) and RPδ6-EGFP(282) (B), containing C-terminal truncated versions of the full-length SIV$_{p17}$ and EGFP ORFs. The right-hand panel shows the results of RT-PCR analysis of total RNA isolated from serial passages of both constructs in HeLa cells. Arrowheads indicate the amplification product from the full-length expression vector constructs.

naviruses (Fig. 5A, compare Fig. 2A). Two expression vectors (RPδ6-SIV$_{p17}$-acc and RPδ6-SIV$_{p17}$-aag) were constructed differing only in the sequence of two nucleotides immediately upstream the initiating AUG codon (. . .ac-c**aug**. . . vs . . .aag**aug**. . .) (Fig. 5). Both sequences placed the initiating codon in Kozak context and maintained the predicted overall structure of the AUG loop. However, in the RPδ6-SIV$_{p17}$-acc construct, the ACC triplet disrupted base-pairing that was predicted to increase the stability of the stem-loop formed by SIV$_{p17}$ sequences in the RPδ6-SIV$_{p17}$-aag construct (Figs. 5A and C).

After transfection of HeLa cells with in vitro RNA tran-

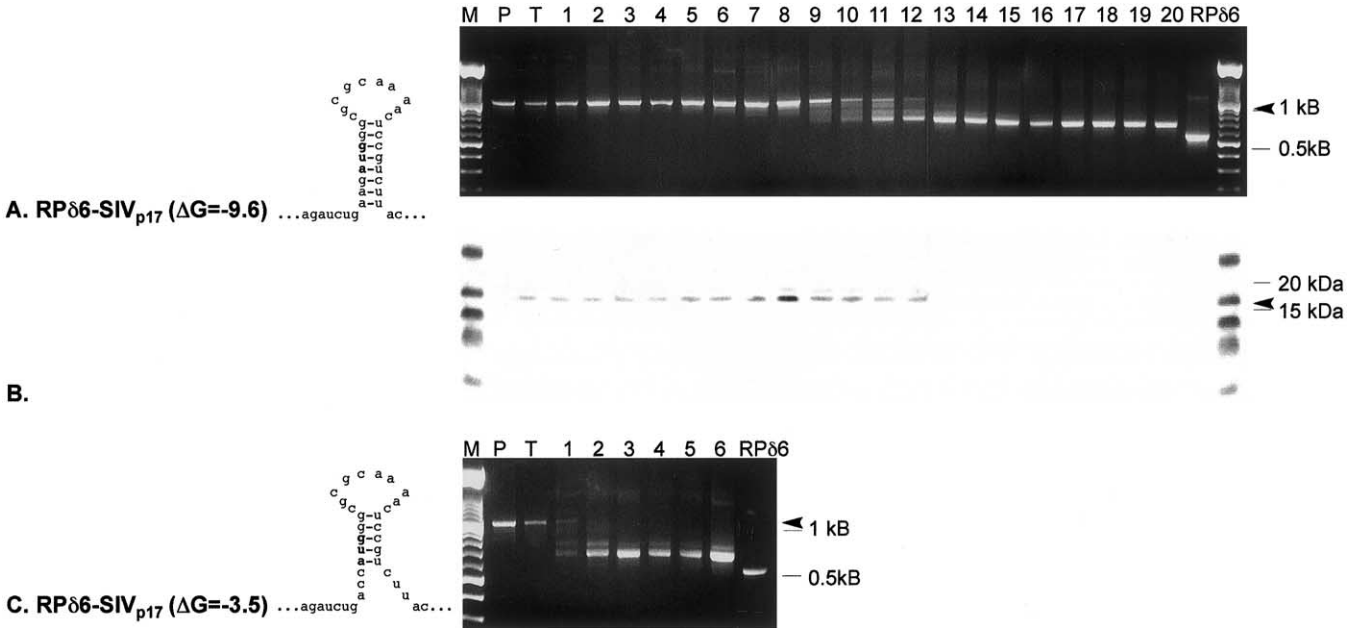

Fig. 5. Effect of the predicted secondary structure of the artificial stem-loop domain VI on insert retention in RPδ6-SIV$_{p17}$. The general architecture of expression construct RPδ6-SIV$_{p17}$ is shown in more detail in Fig. 3. The modified predicted stem-loop structure of the SIV "AUG" loop in RPδ6-SIV$_{p17}$-acc is shown [compare (A) and (C)]. The free energy of the AUG loop formation in constructs RPδ6-SIV$_{p17}$-aag (ΔG = −9.6 kcal/mol) and RPδ6-SIV$_{p17}$-acc (ΔG = −3.5 kcal/mol) was calculated using the Mfold 3.1 algorithm (Zuker et al., 1999). Genetic stability and insert retention was analyzed by RT-PCR of total RNA isolated from serial passages of the corresponding virus. The labeling of lanes in the agarose gels is as shown in Fig. 3. Arrowheads point toward the full-length SIV$_{p17}$ insert. (A) Serial passaging of RPδ6-SIV$_{p17}$-aag yielded a number of deletion variants by the 9th passage. (B) SIV$_{p17}$ could be detected by Western blot of infected cell lysates up to the 12th passage (arrowhead). (C) Deletion of foreign insert was significantly accelerated by the decreased predicted stability of the SIV AUG loop in RPδ6-SIV$_{p17}$-acc.

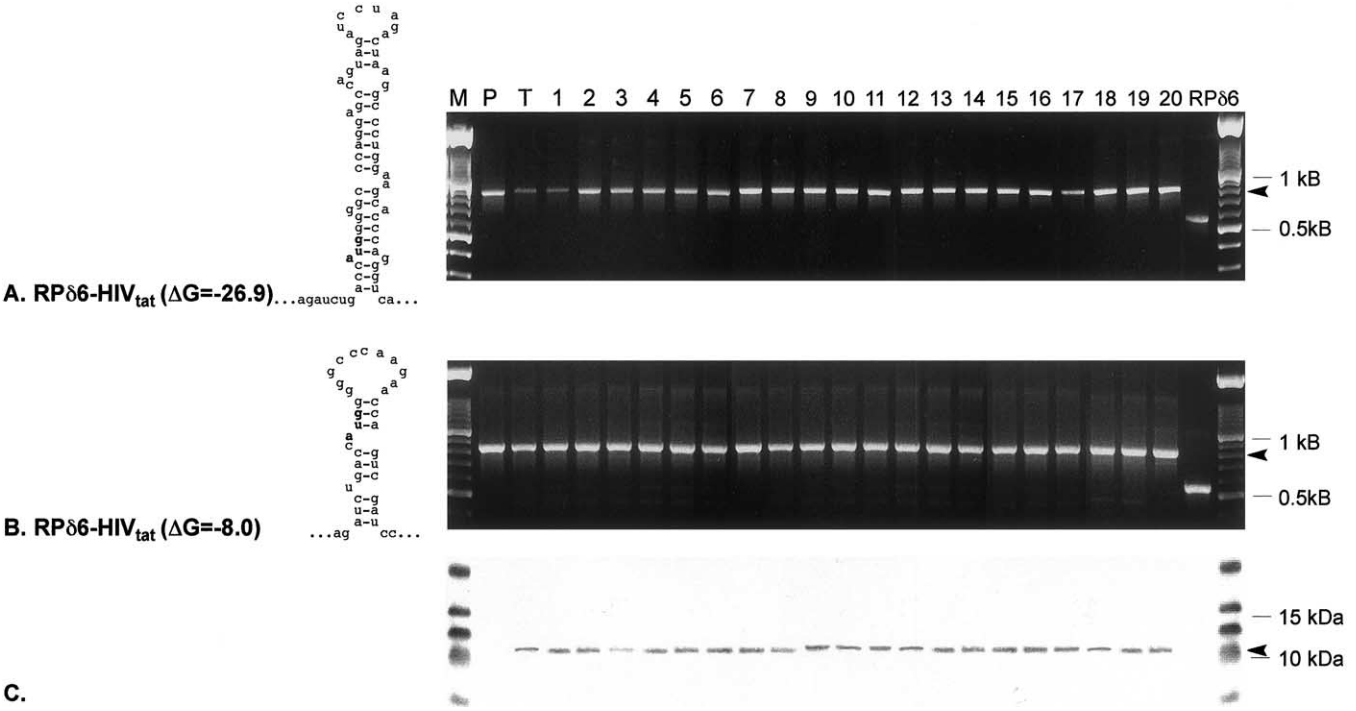

Fig. 6. Genetic stability of RPδ6-HIV$_{tat}$(1) and RPδ6-HIV$_{tat}$(2) expression vectors. The general architecture of RPδ6-HIV$_{tat}$ is shown in detail in Fig. 3. The sequence of HIV$_{tat}$ was modified through silent mutagenesis to form a strong (A; ΔG = −26.9 kcal/mol) or a moderately strong (B; ΔG = −8.0 kcal/mol) stem-loop structure in place of IRES domain VI. Sequence modifications designed to lessen the predicted stability of the artificial stem-loop domain VI did not affect the position of the initiating AUG, the leader peptide, or the overall size of the insert. RT-PCR analysis of serial passages of RPδ6-HIV$_{tat}$(1) and RPδ6-HIV$_{tat}$(2) viruses in HeLa cells is shown on the right (labeling corresponds to the legend in Fig. 3). Arrowheads indicate the amplicon corresponding to a full-length HIV$_{tat}$ insert. (C) Western blot analysis of cell lysates from serial passages of RPδ6-HIV$_{tat}$(1) virus with HIV$_{tat}$-specific antibodies (the arrowhead indicates HIV$_{tat}$).

scripts, we recovered viruses that were subjected to serial passages in HeLa cells. Total cellular RNA was isolated from each infected culture and analyzed by RT-PCR with virus-specific primers encompassing the IRES and SIV$_{p17}$ insert (Fig. 5).

RT-PCR analysis revealed a significantly decreased retention of the foreign ORF in RPδ6-SIV$_{p17}$-acc, due to the minor alteration resulting in weakening of the recombinant stem-loop domain VI (Fig. 5C). RPδ6-SIV$_{p17}$-acc displayed deletions of SIV$_{p17}$ sequences already after the first passage after transfection (Fig. 5C). Within two passages the intact foreign insert could no longer be detected by RT-PCR of total RNA isolated from infected cells (Fig. 5C). In contrast, RPδ6-SIV$_{p17}$-aag, merely differing by a slightly more stable stem-loop structure, retained the intact SIV$_{p17}$ insert for at least eight subsequent passages (Fig. 5A). Western blot analysis of cell lysates from consecutive passages of RPδ6-SIV$_{p17}$-aag was consistent with RT-PCR data revealing SIV$_{p17}$ expression in tandem with insert retention (Fig. 5B). SIV$_{p17}$ expression was detected until the 12th passage, when full-length insert could barely be detected by RT-PCR analysis (compare Figs. 5A and B).

Eventually, several deletion mutants emerged with the 9th passage of RPδ6/SIV$_{p17}$-aag and after the 12th passage, full-length insert could no longer be detected by RT-PCR. From the 15th passage on, a sole amplification product remained, retaining 126 nt (~30%) of the original insert.

Our observations, indeed, suggested that secondary structure of foreign sequences inserted to replace IRES domain VI might influence the genetic stability of RPδ6 expression vectors. Constructs with foreign inserts predicted to form stable secondary structure mimicking the architecture of IRES domain VI could have advantages over nonstructured inserts with regard to retention of heterologous sequences.

To corroborate this hypothesis, we modified the predicted stability of stem-loop structures formed by poliovirus expression vectors with stably retained inserts. For this purpose we chose RPδ6-HIV$_{tat}$, stably retaining a 282-bp foreign insert for at least 20 passages (Fig. 3B). Three expression vectors, RPδ6-HIV$_{tat}$(1)–(3), were constructed that contained inserts differing in the predicted stability of the artificial domain VI stem-loop formed by sequences coding for HIV$_{tat}$ (Figs. 6 and 7).

The RPδ6-HIV$_{tat}$(1) and RPδ6-HIV$_{tat}$(2) constructs with strong and moderately strong secondary structures forming stem-loop domain VI (ΔG = −26.9 and −8.0 kcal/mol, respectively, Figs. 6A and B), were stable throughout at least 20 serial passages. A single amplification product corresponding to the full-length HIV$_{tat}$ insert was detected

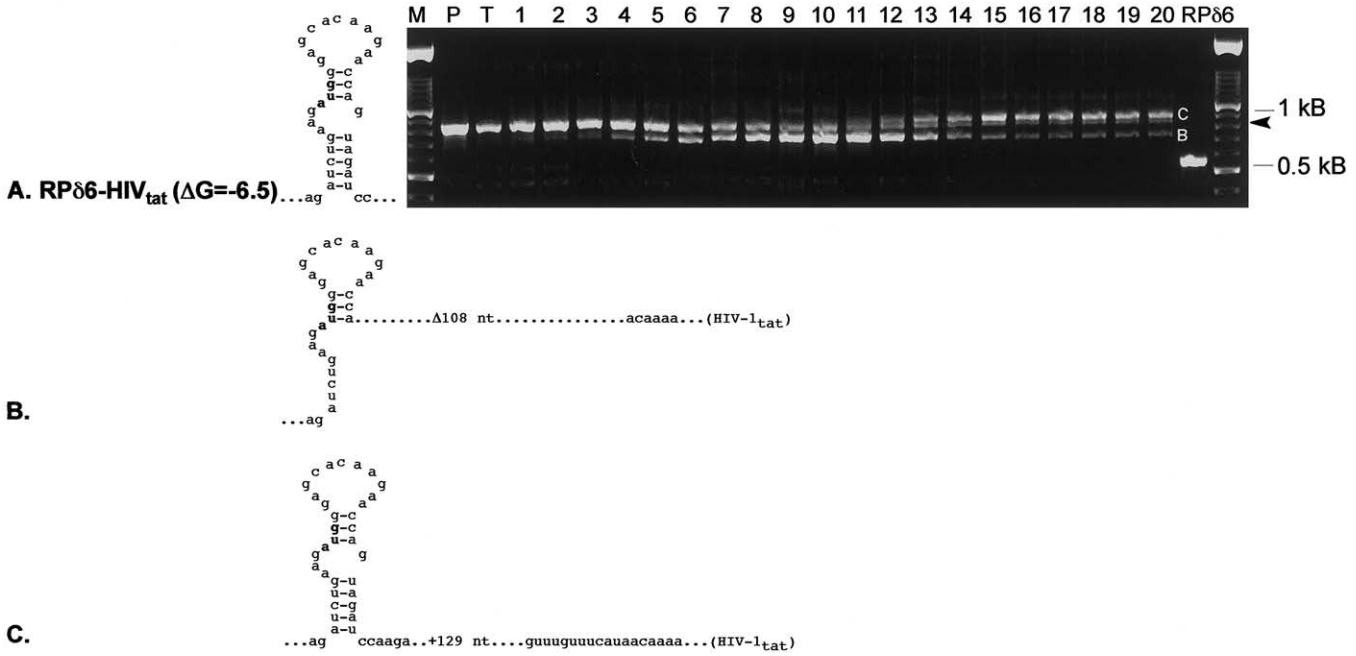

Fig. 7. Genetic stability of RPδ6-HIV$_{tat}$(3). (A) The predicted stability of the artificial stem-loop structure formed by HIV$_{tat}$ sequence in RPδ6-HIV$_{tat}$(1), and (2) was further lowered by silent mutagenesis to yield RPδ6-HIV$_{tat}$(3) (ΔG = −6.5 kcal/mol). RT-PCR analysis of serial passages of RPδ6-HIV$_{tat}$(3) virus in HeLa cells revealed rapid deletion of the foreign insert and the emergence of an enlarged variant (the full-length unaltered insert is indicated by an arrowhead). (B) Genetic structure and sequence of a deletion variant of RPδ6-HIV$_{tat}$(3) isolated at the 10th passage. (C) Genetic structure and sequence of an enlarged RPδ6-HIV$_{tat}$(3) variant isolated at the 20th passage.

by RT-PCR in all passages (Figs. 6A and B). Accordingly, Western blot analysis revealed solid expression of HIV$_{tat}$ in infected cell lysates collected from consecutive passages (Fig. 6C).

In contrast, RPδ6-HIV$_{tat}$(3) (stem-loop VI, ΔG = −6.5 kcal/mol) acquired deletions in the HIV$_{tat}$ insert already after the third passage (Fig. 7A). Notwithstanding the appearance of deletion variants, full-length insert could still be detected after 20 passages (Fig. 7A). Surprisingly, upon appearance of deletion variants, we also detected a variant containing an enlarged insert, emerging after the 11th passage of RPδ6-HIV$_{tat}$(3) in HeLa cells (Fig. 7A). RT-PCR data indicated that the enlarged variant rapidly became predominant in the viral population, evident from the relative intensities of the amplification products. This finding suggested a beneficial effect of insert enlargement leading to increased fitness over RPδ6-HIV$_{tat}$(3) and its deletion variants.

Sequencing of deletion variants emerging upon serial passages of RPδ6-HIV$_{tat}$(3) revealed a 108-nt internal deletion within the ORF for HIV$_{tat}$. This deletion retained all but a remnant stem-loop structure VI (Fig. 7B). Interestingly, sequencing of the enlarged RPδ6-HIV$_{tat}$(3) variant (Fig. 7C) revealed replacement of an internal fragment of 84 nt of the HIV$_{tat}$ ORF with a 129-nt duplication of viral coding sequences for the capsid protein VP1 (nt 2986–3115). These observations conflicted with the expectation of foreign inserts to be deleted to restore efficient growth.

Our observations indicated that foreign sequences inserted strategically to functionally replace secondary structures within the IRES element might be indefinitely retained by replicating virus. These data suggest that high retention rates are achieved because foreign sequence inserts do not either interfere with or even exert beneficial effects on efficient virus propagation. We therefore examined the growth kinetics of a prototype stable poliovirus-based expression vector, RPδ6-HIV$_{tat}$(2), and compared the relative rates of viral gene expression and foreign insert expression (Fig. 8).

Comparative one-step growth curves of RPδ6-HIV$_{tat}$(2) and its parent RPδ6 demonstrated viral growth rates slightly accelerated with the former (Fig. 8A). The analysis of foreign gene expression with HIV$_{tat}$-specific antibodies revealed high expression rates of the foreign insert in step with those of cognate viral gene products (Fig. 8B). The data shown demonstrated efficient synthesis of the fusion polyprotein containing the foreign ORF and uninhibited proteolytic processing at the artificial 2A^{pro} site (no unprocessed precursors of the foreign gene product were detected).

Viral gene expression of RPδ6-HIV$_{tat}$(2), measured through detection of the viral nonstructural protein 2C and its proteolytic precursors P2 and 2BC (Fig. 8B), occurred earlier than with RPδ6. Initial viral gene expression of RPδ6-HIV$_{tat}$(2) was detected already at 3 h p.i., whereas RPδ6 translation occurred with 1 h delay (Fig. 8B).

These observations indicated that, indeed, insertion of foreign sequences in place of HRV2 IRES stem-loop do-

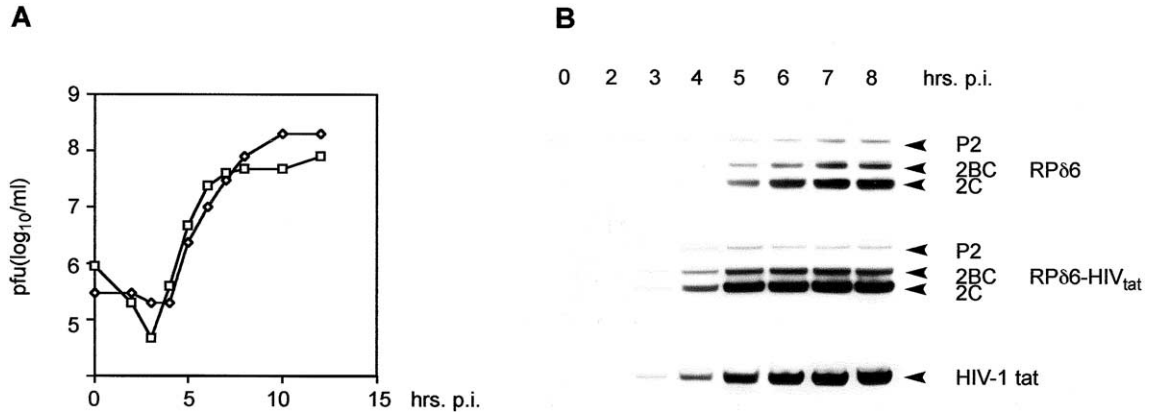

Fig. 8. Comparative rates of virus growth and gene expression in HeLa cells infected with RPδ6 and RPδ6-HIV$_{tat}$(2), respectively. At the indicated time points [(0, 2, 3, 4, 5, 6, 7, and 8 h postinfection (p.i.)] infection was interrupted and freeze-thawed cell lysates were subjected to plaque assay or Western blot analysis as described under Materials and methods. (A) One-step growth kinetics of RPδ6 (open diamonds) and RPδ6-HIV$_{tat}$(2) (open squares). (B) Western blot analysis of RPδ6 (top) and RPδ6-HIV$_{tat}$(2) (middle) with monoclonal antibodies against the poliovirus P2/2BC/2C gene products. The bottom represents Western blot analysis of RPδ6-HIV$_{tat}$(2) with polyclonal antibodies directed against the HIV-1 tat protein. Arrowheads indicate the viral gene products P2, 2BC, and 2C and the HIV-1 tat protein.

main VI confers a growth advantage to RPδ6-HIV$_{tat}$(2). This beneficial effect on viral gene expression may explain long-term retention of foreign sequences in genetically stable picornavirus expression vectors with recombinant IRES elements.

Discussion

Picornaviruses, despite their genetic austerity, devote almost 10% of their coding capacity to the IRES element. These complex, highly structured genetic elements are known to mediate cap-independent initiation of translation (Jang et al., 1988, 1989; Pelletier et al., 1988; Pelletier and Sonenberg, 1988) but also are likely to participate in other functions, e.g., genome replication (Borman et al., 1994).

Structural complexity has hampered efforts to elucidate the functional significance of IRES structure and basic mechanisms of translational initiation at the IRES element. Studies of the effect of mutations on IRES function helped to outline sequence motifs exquisitely sensitive to sequence alterations (Pestova et al., 1991; Belov et al., 1995), but did little to increase our knowledge of basic IRES function. Researchers are faced with the dilemma of a complex three-dimensional structure that may be affected by sequence modification in unforeseen ways.

Picornavirus IRESs have been divided into type 1 (entero-, rhinovirus) and type 2 (aphtho-, hepato-, cardiovirus) (reviewed in Wimmer et al., 1993). All type 1 IRESs are structurally highly related with the exception of the 3′-most portion. Enteroviruses contain a stretch (124–155 nt in length) of predicted unstructured sequence separating stem-loop domain VI from the initiating AUG. Rhinovirus IRES elements lack this “spacer” and, instead, initiate translation from an AUG at the base of stem-loop domain VI (see Fig. 2). The functional significance of the spacer region for enteroviruses is unknown. Deletion of this spacer had no or only negligible effect on poliovirus replication rates in HeLa cells and pathogenicity (Kuge and Nomoto, 1987). Notwithstanding the empirical observations stemming from deletion experiments, the fact that all enteroviruses retain a lengthy spacer region to separate stem-loop domain VI from the initiating AUG may indicate that it is beneficial to virus propagation.

Our observations confirm this assumption, supported by data that showed RPδ6-HIV$_{tat}$(3) virus to acquire a 129-nt insert within the foreign ORF derived of viral sequences coding for VP1 upon serial passages in HeLa cells. Acquisition of added sequence, a rare event in (+)-strand RNA viruses keen on minimizing the length of their genomes, may indicate an increase in viral fitness due to this event. We speculate that a certain structural arrangement surrounding the conserved cryptic AUG (used as initiation codon in our vectors) and the true initiation codon (153 nt downstream of the cryptic AUG in poliovirus) promotes translational initiation. Our data suggest that genetic manipulations which disturb this arrangement, for example, foreign inserts in between both AUG triplets, may trigger adaptation events, e.g., acquisition of added sequences, to restore the preferred structure. Analyses of the secondary structure of added sequences in the enlarged variant of RPδ6-HIV$_{tat}$(3) did not reveal a particular arrangement favored by replicating virus.

Given the intricate relationship of IRES structure and function, we were surprised to observe that substantial alterations of IRES composition, the replacement of an entire stem-loop structure with totally unrelated foreign sequences, were readily tolerated by poliovirus. Our observations indicate that, within limits, the function of certain

regions of the IRES may be maintained by structurally related sequence elements with heterologous sequence.

This principle can be exploited for the construction of genetically stable picornavirus expression vectors. In these vectors, foreign ORFs are retained by replicating virus to functionally replace 5′ noncoding sequences. This vector design bears resemblance to the context of the IRES of hepatitis C virus (HCV). Sequences coding for the HCV core protein located immediately downstream of the initiation codon have been reported to strongly influence IRES function (Lu and Wimmer, 1996; Wang et al., 2000). The influence of core coding sequences on HCV IRES function has been ascribed to structural formations within the core sequence rather than its translation product (Wang et al., 2000).

Attempts to utilize plus-strand RNA viruses for the construction of immunization vehicles, despite their many advantages for vector design and antigen delivery, were consistently plagued by poor retention of foreign inserts. A number of strategies have been proposed to increase the stability of picornaviral expression vectors, e.g., varying the location of the inserted foreign ORF (see Fig. 1). However, the inherent genetic variability of picornaviruses will prevent any attempt to achieve permanent retention of foreign genetic material by simply adding it to the viral genome.

We currently do not understand the exact structural requirements for efficient initiation of translation at the picornaviral IRES element. This is particularly true for the 3′-most IRES region adjacent to the initiation site, containing highly conserved sequence motifs essential for IRES function and harboring areas of diversity that distinguish IRES elements from different picornavirus genera. However, the apparent high degree of genetic plasticity and the virus' preference for a certain structural arrangement within this region open up a unique opportunity to generate genetically stable picornavirus expression vectors. Integrating foreign ORFs into the IRES element to assume regulatory functions benefiting virus replication may force picornaviruses to permanently retain these sequences within their genomes. This new strategy may find applicability in the design of novel picornavirus-based expression vectors for immunization purposes. We are currently investigating our novel vector prototype for vaccination purposes in experimental animals.

Materials and methods

Cloning of foreign ORF into polioviral expression vector

Construction of the recombinant plasmid expressing foreign ORF was performed in the background of a PVS-RIPO cloning cassette (Gromeier et al., 1996) in which the HRV2 IRES was flanked by unique restriction sites *Eco*RI and *Sac*I. The HRV2 IRES fragment lacking domain VI (IRES-δ6) was generated through PCR with the Expand High Fidelity PCR System (Roche) using primers (1) 5′-GGGAATTCACTTAGAAGTTTTTCAC-3′ and (2) 5′-GGAGATCTAAAGGAAAAAGTGAAACACGG-3′ and PVS-RIPO as template.

An antigenic determinant of a bacterial adhesion molecule, FimH, was PCR-amplified with primers (3) 5′-GAAGATCTGACCATGGGCGCGCAGTGTAAAACCGCCAATGGTACC-3′ and (4) 5′-CCGAGCTCCATATGTTGTGAGACCTTTGACGGGCGCAAGGTTTAC-3′ The PCR fragments were digested with *Eco*RI and *Bgl*II (IRES segment) or *Bgl*II and *Sac*I (the FimH fragment) and ligated into PVS-RIPO cut with *Eco*RI and *Sac*I to yield RPδ6-FimH.

RPδ6-HIV$_{tat}$(1), RPδ6-HIV$_{tat}$(2), and RPδ6-HIV$_{tat}$(3) were constructed as follows: the fragments encoding for HIV$_{tat}$ were PCR-amplified from a full-length HIV-1$_{LAI}$ proviral clone (obtained from the NIH AIDS reagent and reference program) with forward primers (5) 5′-AAGGGCCCAGGAGCCAGTAGATCCTAGACTAGAGCCCTGGAAGCACCCAGGGTCACAGCCT-3′ [RPδ6-HIV$_{tat}$(1)], (6) 5′-CCGGGCCCAGGAACCAGTCGATCCTAGACTAGAGCC-3′ [RPδ6-HIV$_{tat}$(2)], or (7) 5′-GGAGATCTGAAGATGGGAGCACAAGAACCAGTAGATCCAAGACTAGAGCCATGGAAGCACCCCGGAAGTC-3′ [RPδ6-HIV$_{tat}$(3)] and the reverse primer (8) 5′-GGGAGCTCCATATGTTGTGAGACCTTTTTCCTTCGGGCCTGTCGG-3′. The IRES-δ6 segment for RPδ6-HIV$_{tat}$(1) and RPδ6-HIV$_{tat}$(2) was generated with primers (1) and (9) 5′-CTGGGCCCCATGGTCAGATCTAAAGGAAAAAGTGAAACACG-3′ and ligated with the corresponding HIV$_{tat}$ fragments through an *Apa*I restriction site. The IRES-δ6 fragment for RPδ6-HIV$_{tat}$(3) was produced with primers (1) and (2) using a *Bgl*II site for the junction with the HIV$_{tat}$ fragment.

RPδ6-SIV$_{p17}$-acc and RPδ6-SIV$_{p17}$-aag, containing the ORF for SIV$_{p17}$, were PCR-amplified from full-length cDNA for SIVmac239 (kindly provided by L. Alexander) with the forward primers (10) 5′-GGAGATCTGACCATGGGCGCGCAAAACTCCGTCTTGTCAGGG-3′ or (11) 5′-GGAGATCTGAAGATGGGCGCGCAAAACTCCGTCTTGTCAGGG-3′ and reverse primer (12) 5′-CCGAGCTCCATATGTTGTGAGACCTTTGTAATTTCCTCCTCTGCCGC-3′ and cloned into PVS-RIPO along with the IRES-δ6 fragment generated with primers (1) and (2). RPδ6-SIV$_{p17}$(282) was generated by PCR amplification of a C-terminally truncated SIV$_{p17}$ fragment using primers (11) and (13) 5′-GGGAGCTCCATATGTTGTGAGACCTTTGATGACGCAGACAGTATTATAAAGG-3′ and inserted into PVS-RIPO as described for the full-length SIV$_{p17}$ fragment.

RPδ6-EGFP was generated by PCR amplification of the insert from pEGFP-N1 (Clontech Laboratories, Inc.) with primers (14) 5′-CCGTGCACAGGTCTCCAAGGGAGAGGAGCTGTTC-3′ and (15) 5′-GGGAGCTCCATATGTTGTGAGACCTTTCTTGTACAGCTCGTCCATGC-3′. For this expression vector, domains II–V of the HRV2 IRES were amplified with primers (1) and (16) 5′-CCGTGCACCCATGTTCAAATATAAAGGAAAA-3′. The ligation of the IRESδ6 and EGFP fragments was accomplished through

an *Apa*LI site introduced by a silent mutation. The truncated EGFP fragment in RPδ6-EGFP(282) was PCR-amplified using primers (14) and (17) 5′-GGGAGCTCCATATGTT-GTGAGACCTTTGAAGAAGTCGTGCTGCTTC-3′ and inserted into PVS-RIPO as described.

Recovery of infectious virus and passaging

Recombinant plasmids containing viral cDNA were digested at a unique *Avi*II site, purified using a PCR Purification Kit (Qiagen), and used as templates for in vitro transcription that was performed with T7 RNA polymerase (Stratagene) as described before (Gromeier et al., 1996). RNA from in vitro transcription reactions was quantified through parallel agarose gel electrophoresis with a quantitation standard (Invitrogen). The integrity of transcript RNA was determined through analytic gel electrophoresis in 0.7% agarose, 6% formaldehyde, 1× MOPS buffer (0.1 M MOPS, pH 7.0, 40 mM sodium acetate, 5 mM EDTA). Transcript RNA was used at a concentration of 2 pg/cell for transfection experiments. These were carried out by adding the appropriate amount of RNA transcript to 5×10^5 HeLa R19 cells using DMRIE-C Reagent (Gibco) following the manufacturer's instructions. Two days posttransfection, the cells were lysed by two freeze-thaw cycles to produce initial viral stocks.

The recovered virus stocks were subjected to 20 subsequent passages in HeLa cells. For this purpose, the original stock and all subsequent passages were subjected to plaque analysis to determine the viral titer. All passages with all expression constructs were carried out at a multiplicity of infection (m.o.i.) of 5. Briefly, 90% confluent cell monolayers ($\sim 8 \times 10^5$ cells) were incubated with the viral stock at an m.o.i. of 5 for 30 min at room temperature. Then cells were overlaid with growth medium containing 2% FBS and incubated at 37°C for 24 h; following this incubation period, complete CPE had occurred in all passages conducted. Infected cells were lysed by two freeze-thaw cycles. The cell lysate was divided, subjected to plaque assay analysis, and used to establish infection of a fresh cell culture and to collect total cellular RNA for further analysis by RT-PCR. All transfections and subsequent passaging series were performed in duplicate.

RT-PCR analysis of RNA from infected cells

The genetic stability of viruses expressing foreign ORFs was analyzed by reverse transcription–PCR (RT-PCR) of total cellular RNA preparations from infected cell lysates. Total cellular RNA from infected HeLa lysates was isolated using Trizol reagent (Gibco-BRL). Reverse transcription of viral RNA was performed with StrataScript RT Kit (Stratagene) or M-MLV reverse transcriptase (Gibco-BRL) following the manufacturer's instructions. RT reactions were carried out using poliovirus type 1 specific primer (18) 5′-CATGTGCGCCCACTTTCTGTG-3′ complementary to the sequences coding for the capsid protein VP4, immediately downstream of the artificial cleavage site for $2A^{pro}$, separating the foreign ORF from the viral polyprotein. After incubation for 1 h at 42°C, the RT reactions were terminated by incubation for 3 min at 95°C and resulting cDNA was PCR amplified with primers (18) and (19) 5′-CGCCT-GTTTTATACTCCCTTCCC-3′ (annealing to sequences upstream of the IRES element within the cloverleaf) using Taq DNA polymerase (Promega).

One-step virus growth curves

One-step virus growth curves were performed as described in Gromeier et al. (1996). Briefly, HeLa cell monolayers were incubated and gently rocked for 30 min at room temperature with virus to be tested suspended at an m.o.i. of 10. Thereupon, monolayer cultures were thoroughly rinsed three times to remove unbound virus and subsequently placed at 37°C for specified periods. Thereafter, the cultures were frozen and treated for further testing by plaque analysis. A 0 h sample, reflecting the portion of virus bound to the cells, was frozen immediately upon removal of unbound particles.

Western blotting

Western blot analysis was used to evaluate foreign gene expression and to compare the relative rates of polioviral and foreign protein synthesis in HeLa cells. Cell monolayers were incubated with virus to be tested at a multiplicity of infection of 10 for 30 min at room temperature. Afterward, cells were washed from unbound virus, overlaid with growth medium containing 2% FBS, and placed at 37°C. At the specified time points infection was interrupted, cells were washed with PBS and lysed with 0.1 ml of SDS–PAGE sample buffer (Invitrogen). Lysed samples (5–10 μl of cell lysate) were resolved by electrophoresis in a 4–12% Bis–Tris NuPAGE Gel (Invitrogen) and transferred to PROTRAN nitrocellulose membrane (Schleicher & Schuell) following standard procedures. After blocking with 3% nonfat milk in TBST (100 mM Tris, 150 mM NaCl, 0.05% Tween 20, pH 8.0) for 1 h, membranes were incubated with primary antibodies. For assays of viral gene expression, an anti-2BC/2C monoclonal antibody (kindly provided by E. Wimmer) was employed. A polyclonal anti-HIV_{tat} antibody (kindly provided by B. Cullen), and hyperimmune sera from rhesus macaques infected with SHIV were used for the Western blot detection of HIV_{tat} and SIV_{p17}, respectively. Following three washes with TBST, membranes were treated with secondary biotinylated antispecies antibody (Vector Labs), rinsed again, and finally developed with streptavidin-horseradish peroxidase (POD) conjugate (Roche) and visualized with POD-blue substrate (Roche) or ECL Western blotting detection reagents (Amersham).

Acknowledgments

We are grateful to E. Wimmer (State University of New York at Stony Brook), L. Alexander (Yale University), B. Cullen, D. Montefiori, and B. Haynes (Duke University) for infectious clones, antibodies, and hyperimmune monkey sera used in our assays. This research was supported by Public Service Grant CA87537 to M.G. M.G. is a recipient of a Burroughs Wellcome Fund Career Award.

References

Alexander, L., Lu, H.H., Wimmer, E., 1994. Polioviruses containing picornavirus type 1 and/or type 2 internal ribosomal entry site elements: genetic hybrids and the expression of a foreign gene. Proc. Natl. Acad. Sci. USA 91, 1406–1410.

Andino, R., Silvera, D., Suggett, S.D., Achacoso, P.L., Miller, C.J., Baltimore, D., Feinberg, M.B., 1994. Engineering poliovirus as a vaccine vector for the expression of diverse antigens. Science 265, 1448–1451.

Arnold, G.F., Resnick, D.A., Smith, A.D., Geisler, S.C., Holmes, A.K., Arnold, E., 1996. Chimeric rhinoviruses as tools for vaccine development and characterization of protein epitopes. Intervirology 39, 72–78.

Belov, G.A., Gmyl, A.P., Maslova, S.V., Pilipenko, E.V., Agol, V.I., 1995. The critical significance of a conserved single-stranded interdomain linker in the 5′-untranslated region of poliovirus RNA. Mol. Biol. (Mosk.) 29, 294–300.

Berkhout, B., 1996. Structure and function of the human immunodeficiency virus leader RNA. Prog. Nucleic Acid Res. Mol. Biol. 54, 1–34.

Borman, A.M., Deliat, F.G., Kean, K.M., 1994. Sequences within the poliovirus internal ribosome entry segment control viral RNA synthesis. EMBO J. 13, 3149–3157.

Burke, K.L., Dunn, G., Ferguson, M., Minor, P.D., Almond, J.W., 1989. A cassette vector for the construction of antigen chimeras of poliovirus. J. Gen. Virol. 70, 2475–2479.

Choi, W.S., Pal-Gosh, R.S., Morrow, C.D., 1991. Expression of human immunodeficiency virus type 1 (HIV-1) Gag, Pol, and Env proteins from chimeric HIV-1 poliovirus minireplicons. J. Virol. 65, 2875–2883.

Crotty, S., Lohman, B.L., Lu, F.X., Tang, S., Miller, C.J., Andino, R., 1999. Mucosal immunization of cynomolgus macaques with two serotypes of live poliovirus vectors expressing simian immunodeficiency virus antigenes: stimulation of humoral, mucosal, and cellular immunity. J. Virol. 73, 9485–9495.

Crotty, S., Miller, C.J., Lohman, B.L., Neagu, M.R., Compton, L., Lu, D., Lu, F.X., Fritts, L., Lifson, J.D., Andino, R., 2001. Protection against simian immunodeficiency virus vaginal challenge by using Sabin poliovirus vectors. J. Virol. 75, 7435–7452.

Dufresne, A.T., Dobrikova, E., Schmidt, S., Gromeier, M., 2002. Genetically stable picornavirus expression vectors with recombinant internal ribosomal entry sites. J. Virol. 76, 8966–8972.

Evans, D.J., McKeating, J., Meredith, J.M., Burke, K.L., Katrak, K., John, A., Ferguson, M., Minor, P.D., Weiss, R.A., Almond, J.W., 1989. An engineered poliovirus chimera elicits broadly reactive HIV-1 neutralizing antibodies. Nature 339, 385–388.

Gromeier, M., Alexander, L., Wimmer, E., 1996. Internal ribosomal entry site substitution eliminates neurovirulence in intergeneric poliovirus recombinants. Proc. Natl. Acad. Sci. USA 93, 2370–2375.

Gromeier, M., Bossert, B., Arita, M., Nomoto, A., Wimmer, E., 1999. Dual stem loops within the poliovirus internal ribosomal entry site control neurovirulence. J. Virol. 73, 958–964.

Gromeier, M., Lachmann, S., Rosenfeld, M.R., Gutin, P.H., Wimmer, E., 2000. Intergeneric poliovirus recombinants for the treatment of malignant glioma. Proc. Natl. Acad. Sci. USA 97, 6803–6808.

Gromeier, M., Lu, H.H., Alexander, L., Wimmer, E., 1997. Attenuated poliovirus as live vector, in: Levine, M.M. (Ed.), New Generation Vaccines, Second ed., Marcel Dekker Inc., New York, pp. 315–329.

Gromeier, M., Nomoto, A., 2002. Pathogenesis of Picornaviruses, in: Semler, B., Wimmer, E. (Eds.), Picornaviruses, Academic Press, Oxford.

Halim, S.S., Ostrowski, S.E., Lee, W.T., Ramsingh, A.I., 2001. Immunogenicity of a foreign peptide expressed within a capsid protein of an attenuated coxsackievirus. Vaccine 19, 958–965.

Iizuka, N., Kohara, M., Hagino-Yamagishi, K., Abe, S., Komatsu, T., Tago, K., Arita, M., Nomoto, A., 1989. Construction of less neurovirulent polioviruses by introducing deletions into the 5′ noncoding sequence of the genome. J. Virol. 63, 5354–5363.

Jang, S.K., Davies, M.V., Kaufman, R.J., Wimmer, E., 1989. Initiation of protein synthesis by internal entry of ribosomes into the 5′ nontranslated region of encephalomyocarditis virus RNA in vivo. J. Virol. 63, 1651–1660.

Jang, S.K., Kräusslich, H.G., Nicklin, M.J., Duke, G.M., Palmenberg, A.C., Wimmer, E., 1988. A segment of the 5′ nontranslated region of encephalomyocarditis virus RNA directs internal entry of ribosomes during in vitro translation. J. Virol. 62, 2636–2643.

Kozak, M., 1999. Initiation of translation in prokaryotes and eukaryotes. Gene 234, 187–208.

Kuge, S., Nomoto, A., 1987. Construction of viable deletion and insertion mutants of the Sabin strain of type 1 poliovirus: function of the 5′ noncoding sequence in viral replication. J. Virol. 61, 1478–1487.

Lu, H.H., Alexander, L., Wimmer, E., 1995. Construction and genetic analysis of dicistronic polioviruses containing open reading frames for epitopes of human immunodeficiency virus type 1 gp120. J. Virol. 69, 4797–4806.

Lu, H.H., Wimmer, E., 1996. Poliovirus chimeras replicating under the translational control of genetic elements of hepatitis C virus reveal unusual properties of the internal ribosomal entry site of hepatitis C virus. Proc. Natl. Acad. Sci. USA 93, 1412–1417.

Meerovitch, K., Nicholson, R., Sonenberg, N., 1991. In vitro mutational analysis of cis-acting RNA translational elements within the poliovirus type 2 5′ untranslated region. J. Virol. 65, 5895–5901.

Melnick, J.L., 1993. Live attenuated poliovaccines, in: Plotkin, S.A., Mortimer Jr., E.A. (Eds.), Vaccines, second ed., The W.B. Saunders Co., Philadelphia, PA, pp. 155–204.

Mueller, S., Wimmer, E., 1998. Expression of foreign proteins by poliovirus polyprotein fusion: analysis of genetic stability reveals rapid deletions and formation of cardioviruslike open reading frames. J. Virol. 72, 20–31.

Pelletier, J., Kaplan, G., Racaniello, V.R., Sonenberg, N., 1988. Cap-independent translation of poliovirus mRNA is conferred by sequence elements within the 5′ noncoding region. Mol. Cell Biol. 8, 1103–1112.

Pelletier, J., Sonenberg, N., 1988. Internal initiation of translation of eukaryotic mRNA directed by a sequence derived from poliovirus RNA. Nature 334, 320–325.

Pestova, T.V., Hellen, C.U., Wimmer, E., 1991. Translation of poliovirus RNA: role of an essential *cis*-acting oligopyrimidine element within the 5′ nontranslated region and involvement of a cellular 57-kilodalton protein. J. Virol. 65, 6194–6204.

Pestova, T.V., Hellen, C.U., Wimmer, E., 1994. A conserved AUG triplet in the 5′ nontranslated region of poliovirus can function as an initiating codon in vitro and in vivo. Virology 204, 729–737.

Pilipenko, E.V., Blinov, V.M., Chernov, B.K., Dmitrieva, T.M., Agol, V.I., 1989a. Conservation of the secondary structure elements of the 5′-untranslated region of cardio- and aphthovirus RNAs. Nucleic Acids Res. 17, 5701–5711.

Pilipenko, E.V., Blinov, V.M., Romanova, L.I., Sinyakov, A.N., Maslova, S.V., Agol, V.I., 1989b. Conserved structural domains in the 5′-untranslated region of picornaviral genomes: an analysis of

the segment controlling translation and neurovirulence. Virology 168, 201–209.

Pilipenko, E.V., Gmyl, A.P., Maslova, S.V., Svitkin, Y.V., Sinyakov, A.N., Agol, V.I., 1992. Prokaryotic-like *cis* elements in the cap-independent internal initiation of translation on picornavirus RNA. Cell 68, 119–131.

Porter, D.C., Ansardi, D.C., Morrow, C.D., 1995. Encapsidation of poliovirus replicons encoding the complete human immunodeficiency virus type 1 *gag* gene by using a complementation system which provides the P1 capsid protein in *trans*. J. Virol. 69, 1548–1555.

Skinner, M.A., Racaniello, V.R., Dunn, G., Cooper, J., Minor, P.D., Almond, J.W., 1989. New model for the secondary structure of the 5′ non-coding RNA of poliovirus is supported by biochemical and genetic data that also show that RNA secondary structure is important in neurovirulence. J. Mol. Biol. 207, 379–392.

Tang, S., van Rij, R., Silvera, D., Andino, R., 1997. Toward a poliovirus-based simian immunodeficiency virus vaccine: correlation between genetic stability and immunogenicity. J. Virol. 71, 7841–7850.

Wang, T.H., Rijnbrand, R.C., Lemon, S.M., 2000. Core protein-coding sequence, but not core protein, modulates the efficiency of cap-independent translation directed by the internal ribosome entry site of hepatitis C virus. J. Virol. 74, 11347–11358.

Wimmer, D., Hellen, C.U., Cao, X.M., 1993. Genetics of poliovirus. Annu. Rev. Genet. 27, 353–436.

Zuker, M., Mathews, D.H., Turner, D.H., 1999. Algorithms and thermodynamics for RNA secondary structure prediction: a practical guide, in: Barciszewski, J., Clark, B.F.C. (Eds.), RNA Biochemistry and Biotechnology, NATO ASI Series, Kluwer Academic Publishers, Boston, pp. 11–43.